

relative to the ^{14}C -labeled molecules and could thus decrease the $^3\text{H}/^{14}\text{C}$ ratio of **2** relative to the precursor *myo*-inositol.

In conclusion, this study has elucidated several stereochemical aspects of the biosynthesis of the antibiotic spectinomycin, as summarized in Figure 5.

Experimental Section

General Methods and Materials. (6*R*)- and (6*S*)-[4- ^2H ,6- ^3H]glucose were obtained by alkaline phosphatase cleavage²⁰ of the corresponding glucose 6-phosphates available from earlier work.¹⁹ [1- ^3H]-, [4- ^3H]-, [6- ^3H]-, and [6- ^{14}C]glucose were purchased from Amersham/Searle and bacterial (*E. coli*) alkaline phosphatase was from Sigma. Materials for culture media were from Difco Laboratories, except for phytone which was obtained from B.B.L. Purification of (6*R*)- and (6*S*)-[4- ^2H , 6- ^3H]glucose was carried out by preparative TLC on 1-mm cellulose plates, 20 cm \times 20 cm (Brinkmann, precoated), and on 0.25-mm cellulose plates, 20 cm \times 20 cm (Eastman, precoated), using as the solvent system $\text{BuOH}:\text{AcOH}:\text{H}_2\text{O} = 12:3:5$.

Radioactivity was measured in a Beckman LS-7000 scintillation counter in 15 mL of Bray's solution, except for actinamine, which was counted in 10 mL of Aquasol. [^3H]- and [^{14}C]toluene were used as internal standards to determine counting efficiencies.

Culture Conditions. *Streptomyces flavopersicus* NRRL 2820 was maintained on sterilized soil and seed cultures were prepared by inoculating 100 mL of medium, containing 0.5% phytone, 0.5% yeast extract, 1% glucose, 0.1% Bacto-Casetone, and 0.5% NaCl, with spores on soil particles. The cultures, contained in 500-mL Erlenmeyer flasks, were incubated at 32 $^\circ\text{C}$ on a New Brunswick rotary shaker at 160 rpm for 72 h. Production cultures were inoculated with 2 mL of vegetative inoculum from seed cultures. Based on time-course studies, addition of labeled precursors 24 h after inoculation and harvest of the cultures 24 h later was chosen as the standard condition for the feeding experiments.

The precursors were added to the cultures as Millipore-sterilized aqueous solutions.

Isolation and Purification of Spectinomycin. The cultures were filtered, the filtrate was acidified to pH 6.0 with 0.1 N HCl, and spectinomycin was adsorbed onto a column of ion-exchange resin IRC-50 (Na^+) (20 mL). The resin was washed with 50 mL of water, then eluted with 0.5 N HCl (75 mL). The eluent was adjusted to pH 6.0 with 0.1 N NaOH and evaporated to dryness. The residue was taken up in 5 mL of cold absolute MeOH and filtered from salts; the spectinomycin was recrystallized with carrier (40 mg) from water/acetone until the specific radioactivity and $^3\text{H}/^{14}\text{C}$ ratio were constant.

Degradations of Spectinomycin. The Kuhn-Roth oxidations were carried out as described.³⁰ The chirality analysis of sodium acetate was carried out by the method of Cornforth et al.²¹ and Arigoni and co-workers,²² using essentially Eggerer's procedure.²³

Hydrolysis of **1** to **2**, isolated as the dihydrochloride, was carried out as described by Wiley et al.,⁴ as was the periodate oxidation of **2** to give methylamine, which was trapped and analyzed as the hydrochloride.

Acknowledgment. We thank Dr. T. G. Pridham, USDA Northern Regional Research Laboratory, Peoria, Ill., for the strain of *S. flavopersicus*; Dr. Paul F. Wiley of the Upjohn Company, for a gift of spectinomycin; and Mrs. Janet Weaver of this department for carrying out the chirality analyses of the acetate samples. This work was supported by the National Institutes of Health through NIH Research Grants AI 11172 (to H.G.F.) and CA 17047 (to L.H.H.) and through Fogarty International Fellowship TW 02567 (to O.A.M.).

(30) H. Simon and H. G. Floss, "Bestimmung der Isotopenverteilung in markierten Verbindungen", Springer-Verlag, Berlin, 1967, p 26.

The Relationship between Complex Stability Constants and Rates of Cation Transport through Liquid Membranes by Macrocylic Carriers¹

J. D. Lamb,* J. J. Christensen,* J. L. Oscarson, B. L. Nielsen, B. W. Asay, and R. M. Izatt*

Contribution from the Departments of Chemical Engineering and Chemistry and Contribution No. 198 from the Thermochemical Institute, Brigham Young University, Provo, Utah 84602. Received March 24, 1980

Abstract: The relationship between the rate of carrier-facilitated transport of metal cations through chloroform membranes containing macrocylic ligand carriers and the stability constant of the cation-carrier complex in methanol solution was investigated. Several macrocylic ligand carriers were used in transporting Na^+ , K^+ , Rb^+ , Cs^+ , Ca^{2+} , Sr^{2+} , and Ba^{2+} . For maximum cation transport, an optimum range in value of the cation-carrier complex stability constant was shown to exist. The rate of cation transport decreased rapidly at stability constant values higher or lower than this range. The maximum observed transport occurred for carriers having $\log K_{\text{MeOH}}$ values from 5.5 to 6.0 for K^+ and Rb^+ and 6.5 to 7.0 for Ba^{2+} and Sr^{2+} . For all cations, little or no transport occurred with carriers having $\log K_{\text{MeOH}}$ less than 3.5-4.0. An equation was derived which correctly predicts the observed variation of cation transport rate with $\log K_{\text{MeOH}}$ over a wide range of $\log K_{\text{MeOH}}$ values. This equation makes possible the estimation of either $\log K$ or cation-transport rate in certain cases if the other of the two values is known.

Introduction

Macrocylic ligands such as crown ethers and their derivatives (Figure 1, 1-7, 9-11) and cryptands (Figure 1, 12-13) have been used as cation-transport carriers in hydrophobic liquid membranes.²⁻⁹ A liquid membrane system based on the Schulman

bridge has provided a simple means to study transport of this type.^{2,3,5-7,9} In this system, the macrocylic carrier, dissolved in the membrane, facilitates the transport of salt from the source phase through the membrane to the receiving phase by solubilizing the cation into the membrane solvent. In a continuing program to quantitatively describe the factors which influence cation

(1) This work was funded by U.S. Department of Energy Contract No. DE-AS02-78ER05016.

(2) Lamb, J. D.; Christensen, J. J.; Izatt, S. R.; Bedke, K.; Astin, M. S.; Izatt, R. M. *J. Am. Chem. Soc.* **1980**, *102*, 3399-3403.

(3) Wong, K. H.; Yagi, K.; Smid, J. *J. Membr. Biol.* **1974**, *18*, 379-397.

(4) Caracciolo, F.; Cussler, E. L.; Evans, D. F. *AIChE J.* **1975**, *21*, 160-167.

(5) Christensen, J. J.; Lamb, J. D.; Izatt, S. R.; Starr, S. E.; Weed, G. C.; Astin, M. S.; Stitt, B. D.; Izatt, R. M. *J. Am. Chem. Soc.* **1978**, *100*, 3219-3220.

(6) Reusch, C. F.; Cussler, E. L. *AIChE J.* **1973**, *19*, 736-741.

(7) Kobuke, Y.; Hanji, K.; Horiguchi, K.; Asada, M.; Nakayama, Y.; Furukawa, J. *J. Am. Chem. Soc.* **1976**, *98*, 7414-7419.

(8) Schwind, R. A.; Gilligan, T. J.; Cussler, E. L. In "Synthetic Multidentate Macrocylic Compounds", Izatt, R. M., Christensen, J. J., Eds.; Academic Press: New York, 1978; pp 289-308.

(9) Newcomb, M.; Toner, J. L.; Helgeson, R. C.; Cram, D. J. *J. Am. Chem. Soc.* **1979**, *101*, 4941-4947.

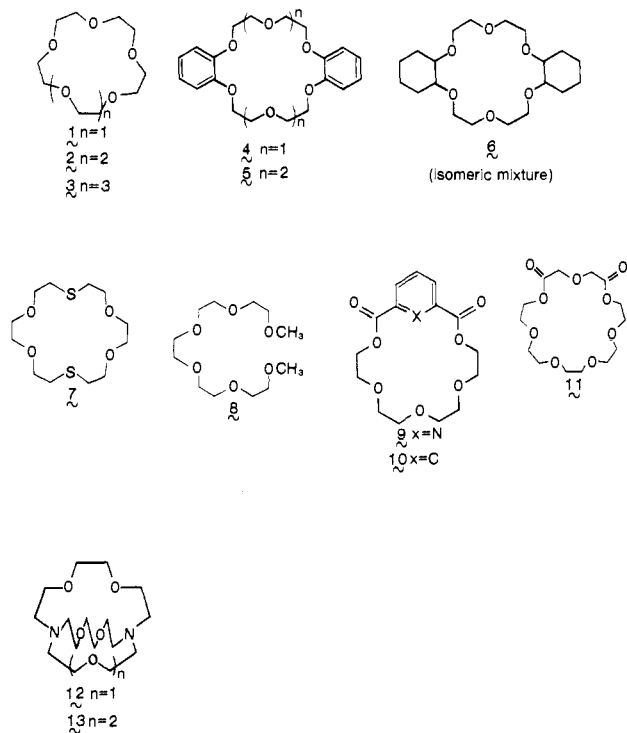


Figure 1. Structures of membrane carrier molecules.

transport of this type, we have shown in previous publications^{2,5} the effect of cation source-phase concentration and of anion type on the transport rates of several cations using macrocyclic crown ether carriers. We here report our results concerning the effect of the stability of the cation-carrier complex on the rate of cation transport.

A characteristic of macrocyclic ligands which makes them desirable membrane carriers is their high degree of cation selectivity. The selectivities of several crown and cryptand ligands have been examined in detail by determining the equilibrium constants for formation of the complexes of several cations, usually in methanol solvent.¹⁰ We have shown that this selectivity is also present in membrane transport systems. For example, high transport selectivity has been achieved for Pb^{2+} over many other cations by using substituted crown ethers.¹¹ It is of interest, therefore, to examine the relationship between thermodynamic and transport selectivities by relating the thermodynamic stability constants for cation-macrocycle complexation and the rates of individual cation transport through liquid membranes containing macrocyclic carriers. That a relationship exists between these two parameters has been demonstrated for a limited number of cases by Kirch and Lehn.¹² We have completed and here report a detailed study of this relationship using several macrocyclic ligand carriers plus pentaglyme with Na^+ , K^+ , Rb^+ , Cs^+ , Ca^{2+} , Sr^{2+} , and Ba^{2+} .

Experimental Section

Liquid membrane experiments were performed in a specially thermostated room ($25 \pm 1^\circ\text{C}$) by using cells which were smaller versions of those described previously.^{2,5} The cells (Figure 2) consisted of a 3.0-mL membrane phase interfaced to both a 0.80-mL source phase (salt solution) and a 5.0-mL receiving phase (distilled deionized water). The membrane phase consisted of reagent grade chloroform (Fisher) containing 0.0010 M carrier and was stirred at 120 rpm by a magnetic stirrer driven by a Hurst synchronous motor. After a period of 24 h, a 3-mL sample of the receiving phase was withdrawn and the number of moles

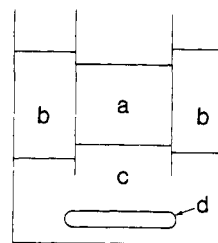


Figure 2. Liquid membrane cell: (a) source phase; (b) receiving phase; (c) membrane phase; (d) magnetic stirring bar.

of cation was determined by either ion chromatography (Dionex Model 10) (Rb^+ , Cs^+ , and Ba^{2+}) or atomic absorption spectrometry (Perkin-Elmer Model 603) (all other cations). It has been shown²⁻⁷ that where the amounts of cation transported are small, the increase in cation concentration in the receiving phase is linear with time.

Three separate cells were used for each salt-macrocycle system to determine the reproducibility of the reported transport rates. Blank experiments (no carrier present) were performed for each source-phase salt solution to determine membrane leakage. The amount of cation leakage varied with cation but was always less than 3×10^{-8} mol/24 h.

Reagent grade compounds 1-8, 12, and 13 (Figure 1) were obtained from Parish Chemical Co. and used without further purification. Compounds 9-11 were synthesized and purified as reported.¹³ Reagent grade nitrate salts were obtained from the following sources: NaNO_3 , KNO_3 (Mallinckrodt); RbNO_3 , CsNO_3 (Alfa-Ventron); $\text{Ca}(\text{NO}_3)_2$ (Baker and Adamson); $\text{Sr}(\text{NO}_3)_2$ (Fisher); $\text{Ba}(\text{NO}_3)_2$ (J. T. Baker). All source-phase solutions were 1.0 M except $\text{Ba}(\text{NO}_3)_2$ which was 0.3 M.

Results and Discussion

The measured values of cation-transport rate using various carriers are presented in Table I. The transport rate J_M is the net metal ion flux across the membrane in 10^{-7} mol/24 h. In addition, $\log K$ data are given in Table I for the 1:1 reaction of the carrier ligands with each of the cations used in the transport experiments. Ideally, these $\log K$ data would be those valid for chloroform saturated with water, since the transport mechanism outlined here predicts that J_M should vary directly with K values valid in the membrane solvent. However, few if any values of $\log K$ have been reported in the membrane solvent, chloroform. Consequently, $\log K$ data are listed in Table I as determined in methanol, the most common solvent of dielectric constant smaller than that of water for which a wide variety of $\log K$ data is available.¹⁰

The variation of macrocyclic complex stability constants with solvent has been treated in detail elsewhere.¹⁰ In particular, the stabilities of cation complexes of 18-crown-6 increase in a regular fashion through a series of water/methanol solvents (see Figure 6 in Izatt et al.¹⁴ and Figure 2 in Izatt et al.¹⁵). Furthermore, $\log K^{10,16}$ data for the reaction of Na^+ , K^+ , and Cs^+ with dicyclohexano-18-crown-6 in a series of pure alcohol solvents of decreasing dielectric constant indicate that $\log K$ increases in a regular fashion with solvent dielectric constant. Although a few exceptions to this relationship are known,^{10,17} these involve solvents whose molecules do not behave as simple dipoles like methanol and chloroform. Thus, for simple solvents like chloroform, methanol and water, there is an empirical basis for assuming that basic trends in the complex stability constants for a given species in one solvent may reflect those in the others. This same assumption was made implicitly by Kirch and Lehn,¹² who first related cation transport rates to $\log K$ values for complex for-

(13) Bradshaw, J. S.; Maas, G. E.; Izatt, R. M.; Christensen, J. J. *Chem. Rev.* 1979, 79, 37-52.

(14) Izatt, R. M.; Hansen, L. D.; Eatough, D. J.; Bradshaw, J. S.; Christensen, J. J. In "Metal-Ligand Interactions in Organic Chemistry and Biochemistry"; Pullman, B., Goldblum, N., Eds.; D. Reidel Publishing Co. Dordrecht, Holland, 1977; Part 1, pp 337-361.

(15) Izatt, R. M.; Terry, R. E.; Nelson, D. P.; Chan, Y.; Eatough, D. J.; Bradshaw, J. S.; Hansen, L. D.; Christensen, J. J. *J. Am. Chem. Soc.* 1976, 98, 7626-7630.

(16) Agostiano, A.; Caselli, M.; Della Monica, M. *J. Electroanal. Chem.* 1976, 74, 95-105.

(17) Matsuura, N.; Umamoto, K.; Takeda, Y.; Sasaki, A. *Bull. Chem. Soc. Jpn.* 1976, 49, 1246-1249.

(10) Lamb, J. D.; Izatt, R. M.; Christensen, J. J.; Eatough, D. J. In "Coordination Chemistry of Macrocyclic Compounds", Melson, G. A., Ed.; Plenum Press: New York, 1979; pp 145-217.

(11) Lamb, J. D.; Izatt, R. M.; Robertson, P. A.; Christensen, J. J. *J. Am. Chem. Soc.* 1980, 102, 2452-2454.

(12) Kirch, M.; Lehn, J. M. *Angew. Chem., Int. Ed. Engl.* 1975, 14, 555-556.

Table I. Rates of Transport, J_M , of Nitrate Salts through a Bulk Chloroform Membrane Containing 1 mM Carrier at 25 °C and log K values for 1:1 Cation-Carrier Complex Formation in Methanol at 25 °C

carrier		Na ⁺	K ⁺	Rb ⁺	Cs ⁺	Ca ²⁺	Sr ²⁺	Ba ²⁺
1	J_M^a	28 ± 5	3.4 ± 0.5	1.0 ± 0.1	0	0	0	3.3 ± 2.0
	log K	3.48 ^b	3.77 ^b		2.18 ^b	2.18 ^b	2.63 ^b	
2	J_M	11.3 ± 0.6	280 ± 30	210 ± 40	34 ± 6	26 ± 1	320 ± 20	18 ± 5
	log K	4.36 ^b	6.06 ^b	5.32 ^b	4.79 ^b	3.86 ^b	5.8 ^c	7.04 ^b
3	J_M	4.8 ± 1.3	67 ± 9	72 ± 8	48 ± 3	4.2 ± 0.4	36 ± 17	41 ± 2
	log K	1.73 ^b	4.22 ^b	4.86 ^b	5.01 ^b		1.77 ^b	5.44 ^b
4	J_M	4.2 ± 0.1	101 ± 3	12 ± 4	1.1 ± 0.4	0	0	1.6 ± 0.3
	log K	4.5 ^d	5.00 ^d		3.55 ^d			4.28 ^d
5	J_M	1.7 ± 0.1	1.9 ± 0.7	3.6 ± 0.7	2.4 ± 1.0	0	0	0.8 ± 0.4
	log K		3.49 ^d	4.0 ^c	3.78 ^d			
6	J_M	23 ± 3	340 ± 70	240 ± 30	32 ± 7	160 ± 5	490 ± 60	300 ± 45
	log K	3.9 ^e	5.7 ^e		4.1 ^e		6.4 ^{e,f}	6.9 ^{e,f}
7	J_M	1.5 ± 0.4	0	0	0	0	0	0.70 ± 0.09
	log K		1.15 ^d					
8	J_M	5 ± 2	0.6 ± 0.2					3.9 ± 1.2
	log K	1.44 ^g	2.27 ^g					2.51 ^g
9	J_M	2.7 ± 0.2	93 ± 11	31 ± 3	0.9 ± 0.2	1.0 ± 0.2	15 ± 5	0
	log K	4.29 ^h	4.66 ^h	4.24 ^h				4.34 ^h
10	J_M	0.65 ± 0.02	0	0	0	0	0	2.4 ± 1.8
	log K	<0.5 ^h	<0.5 ^h	<0.5 ^h	<0.5 ^h	<0.5 ^h	<0.5 ^h	<0.5 ^h
11	J_M	0.7 ± 0.2	0	0.6 ± 0.1	0			0.6 ± 0.1
	log K	2.5 ^h	2.79 ^h	2.09 ^h	2.55 ^h			3.1 ^h
12	J_M	130 ± 40	290 ± 60	550 ± 90	28 ± 17	4.7 ± 0.4	3.0 ± 0.3	7.5 ± 1.2
	log K	8.94 ⁱ	7.55 ⁱ	5.90 ⁱ	4.00 ⁱ	9.71 ⁱ	10.75 ⁱ	9.80 ⁱ
13	J_M	240 ± 9	88 ± 2	205 ± 13	5 ± 1	3.1 ± 0.3	13 ± 2	2.8 ± 0.3
	log K	7.31 ⁱ	9.85 ⁱ	8.50 ⁱ	3.64 ⁱ	7.70 ⁱ	11.6 ⁱ	12 ⁱ

^a Moles transported × 10⁷/24 h from source phase containing 1.0 M nitrate salt, except Ba(NO₃)₂ (0.30 M); reported as average of three independent determinations and standard deviation from average. Where J_M is reported as 0, no more transport was measured than in a "blank" experiment with no carrier present (see Experimental Section). ^b From Lamb et al.¹⁹ ^c Estimated from log K value reported in 70% methanol/30% water by addition of 1.5.¹⁰ ^d From Lamb et al.¹⁰ ^e Average of log K values for isomers a and b; from Lamb et al.¹⁰ ^f Estimated from log K value reported in H₂O¹⁰ by addition of 3.5. ^g From Lamb et al.²⁰ ^h From Lamb et al.²¹ ⁱ Estimated from log K value reported in 95% methanol/5% water¹⁰ by addition of 0.10.

mation. We have found and demonstrate herein that the cation transport rates measured here can be correlated to log K values for the carrier-cation complex in methanol.

From limited results using cryptand carriers, Kirch and Lehn¹² predicted that for cation transport an optimum value of K exists above or below which the rate of transport decreases. Our results, listed in Table I, conform to this hypothesis if we assume that differences in transport rate are primarily due to differences in log K when a common salt is transported and not in other properties of the different ligands such as the diffusion coefficient. In Figure 3 are plotted J_M vs. log K_{MeOH} for each of Na⁺, K⁺, Rb⁺, Cs⁺, Ca²⁺, Sr²⁺, and Ba²⁺, where each point represents the coordinates for transport by and reaction with a different ligand among those in Figure 1. For each cation, J_M is very small at log K values less than 3.5. Where data are available, the J_M values are seen to rise to a maximum and then sharply decrease as log K increases. Unfortunately, for Na⁺, Cs⁺, and Ca²⁺ macrocyclic ligands with log K values of intermediate magnitude were unavailable, so that complete (or nearly so) curves can be provided for K⁺, Rb⁺, Sr²⁺, and Ba²⁺ only. However, the limited data for Na⁺, Cs⁺, and Ca²⁺ also conform to the trends seen for the other cations.

As illustrated in Figure 3, the measured log K value which corresponds to maximum cation transport is between 5.5 and 6.0 for both K⁺ and Rb⁺ and between 6.5 and 7.0 for both Ba²⁺ and Sr²⁺. However, the interpolations made in Figure 3 are for illustrative purposes only; it is conceivable that the true maxima occur at positions on the curves of K⁺, Rb⁺, Sr²⁺, and Ba²⁺ where points are not available. Strictly speaking, therefore, the data do not define the positions of the maxima to within 0.5 log K unit. When the curve for K⁺ is examined, the maximum must lie between log K values of 5.00 (ligand 4) and 6.60 (ligand 2) and it is difficult to discern whether the point at log K_{MeOH} value 5.7 (ligand 6) is on the upward or downward slope or at the maximum proper. By similar reasoning, the maximum in the Rb⁺ curve must occur between log K_{MeOH} values of 5.32 (ligand 2) and 8.50 (ligand 13), in the Sr²⁺ curve between log K_{MeOH} values of 5.8 (ligand 2) and 10.75 (ligand 12), and in the Ba²⁺ curve between the log

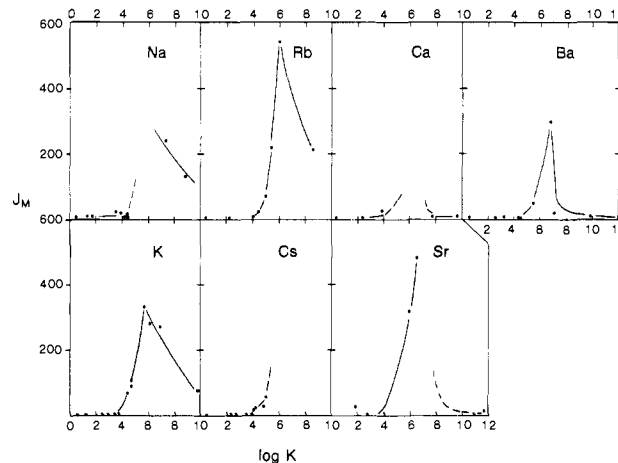


Figure 3. J_M (× 10⁷ mol/24 h) vs. log K_{MeOH} for seven cations. Compare to Table I to determine the membrane carrier represented by each point. Lines (solid and dashed) are included to aid the eye in recognizing trends in the data which are common to all cations.

K_{MeOH} values of 5.44 (ligand 3) and 7.04 (ligand 2). Insufficient data are available to determine the position of the maximum for the other cations studied. Further discussion concerning the position of the maxima in these curves will be undertaken following introduction of a theoretical model to describe these results.

A Theoretical Transport Model

A theoretical basis for relating J_M to the stability constant, K , has been reported by Reusch and Cussler.⁶ The transport mechanism proposed by them has been successfully tested with respect to cation concentration,⁶ cation activity,² ligand concentration,⁶ and anion type.^{2,5} A simplified form (eq 1) of their flux

$$J_M = D_{CK}K_L M_1^2 / l \quad (1)$$

equation (where the variables are defined in footnote 18) predicts

that the metal ion flux, J_M , should vary directly as the equilibrium constant, K , where K applies to reaction 2. In reaction 2, (M^+A^-)



represents the cation associated with its anion after partitioning into the membrane from the source phase, L represents the carrier ligand in the membrane, and (ML^+A^-) represents the cation-ligand complex associated with the anion in the membrane.

The model of Reusch and Cussler as described in eq 1 correctly predicts the exponential rise in J_M in the region of low $\log K$ values as observed in the curves in Figure 3. However, it does not predict the observed decrease in transport rate at high $\log K$ values. A cation-transport model based on similar principles which correctly predicts the change in J_M with $\log K$ over the whole range of $\log K$ values is derived below. A representation of the liquid membrane system used in this theoretical development is given in Figure 4. Vertical lines 2 and 7 represent the interfaces between source and membrane phases and membrane and receiving phases, respectively. The thickness of the water boundary layers on each side of the membrane are given by l_1 and l_6 ; the membrane boundary layer thicknesses are given by $l_2 + l_3$ and $l_4 + l_5$. The parameters l_2 and l_3 represent the mean distance through which the free-ion pair diffuses in the chloroform boundary layer before (on the source side) or after (on the receiving side) reaching equilibrium with carrier. The mechanism of transport is that described in a previous paper² and by Reusch and Cussler.⁶ Specifically, it is assumed that the rates at which cation and anion partition into the receiving phase and at which cation reacts with or is released from carrier ligand are fast compared to diffusion. It is further assumed that (i) the system is at steady state, (ii) the diffusivities in the membrane of the free ligand, D_L , and of the ligand-metal ion complex are equal, and (iii) the bulk velocity of the water boundary layer normal to the membrane interface is zero.

The flux of metal ions through the membrane-source-phase interface J_S and through the membrane-receiving-phase interface J_R are given by eq 3 and 4 (see Figure 4 for location of interfaces

$$J_S = (D_L/l_3)(C_3 - C_4) \quad (3)$$

$$J_R = (D_L/l_4)(C_5 - C_6) \quad (4)$$

1-8), where C represents the molar concentration of the carrier-cation complex associated with anion(s) in the various positions in the membranes. Since at steady state $C_4 = C_5$ and $A_1J_S = A_2J_R$ (where A_1 and A_2 represent the surface areas of the source and receiving interfaces), then

$$J_S = \frac{D_L}{l_3 + (A_1/A_2)l_4}(C_3 - C_6) \quad (5)$$

If the complexation constant K for reaction 2 is defined by eq 6,

$$K = [(ML^+A^-)]/[(M^+A^-)][L] = C_6/L_6I_6 \quad (6)$$

where I represents the molar concentration of the cation-anion pair and the total carrier ligand concentration L_T is represented by eq 7; therefore

$$L_T = L_6 + C_6 \quad (7)$$

(18) J_M = flux of salt across membrane; D_C = diffusion coefficient of complexed salt; k = partition coefficient of salt between water and membrane; K = equilibrium constant for salt-carrier complexation; L_T = total carrier ligand concentration; M_1 = source-phase salt concentration; l = membrane thickness.

(19) Lamb, J. D.; Izatt, R. M.; Swain, C. S.; Christensen, J. J. *J. Am. Chem. Soc.* **1980**, *102*, 475-479.

(20) Lamb, J. D.; Izatt, R. M.; Christensen, J. J.; Haymore, B. L., submitted for publication in *Inorg. Chem.*

(21) Lamb, J. D.; Izatt, R. M.; Swain, C. S.; Bradshaw, J. S.; Christensen, J. J. *J. Am. Chem. Soc.* **1980**, *102*, 479-482.

$$C_6 = KL_T I_6 / (1 + KI_6) \quad (8)$$

Since

$$J_R = (D_1/l_5)(I_6 - I_7) \quad (9)$$

then, combining with eq 8

$$C_6 = \frac{KL_T(I_7 + (J_R l_5 / D_1))}{1 + K(I_7 + (J_R l_5 / D_1))} \quad (10)$$

The partition coefficient for the salt of a monovalent cation between water and membrane is given by eq 11, where M represents

$$k = I_7 / M_7^2 \quad (11)$$

the molar concentration of the metal cation. Substituting eq 11 into equation 10, along with the relationships $J_R = (D_W/l_6)(M_7 - M_8)$, where D_W is the diffusion coefficient of the salt in water, and $A_S J_S = A_R J_R$, we obtain an expression, eq 12, for the concentration of the metal-ligand complex at point 6. In similar

$$C_6 = \frac{KL_T(k(M_8 + (A_1/A_2)(J_S l_6 / D_w))^2 + (A_1/A_2)(J_S l_5 / D_1))}{1 + K(k(M_8 + (A_1/A_2)(J_S l_6 / D_w))^2 + (A_1/A_2)(J_S l_5 / D_1))} \quad (12)$$

fashion, an expression, eq 13, for the concentration of the complex at point 3 is obtained. The total metal ion flux, defined previously

$$C_3 = \frac{KL_T(k(M_1 - (J_S l_1 / D_w))^2 - (J_S l_2 / D_1))}{1 + K(k(M_1 - (J_S l_1 / D_w))^2 - (J_S l_2 / D_1))} \quad (13)$$

as J_M , is equal to J_S and J_R and can be obtained as in eq 14 by combining eq 12 and 13 with eq 3 and where $n = 2$ for monovalent

$$J_M = \frac{D_L K L_T}{l_3 + (A_1/A_2)l_4} \times \left[\frac{(k(M_1 - (J_M l_1 / D_w))^n - (J_M l_2 / D_1))}{1 + K(k(M_1 - (J_M l_1 / D_w))^n - (J_M l_2 / D_1))} - \frac{k(M_8 + (A_1/A_2)(J_M l_6 / D_w))^n + (A_1/A_2)(J_M l_5 / D_1)}{1 + K(k(M_8 + (A_1/A_2)(J_M l_6 / D_w))^n + (A_1/A_2)(J_M l_5 / D_1))} \right] \quad (14)$$

and $n = 3$ for divalent cations. Equation 14 for monovalent cations ($n = 2$) can be expressed as a fifth order polynomial in J_M . However, for computational purposes, it is simpler to use eq 14.

Equation 14 reduces to a form comparable to that given by Reusch and Cussler⁶ (eq 1) under the following conditions. At small values of k and J_M , the denominators in the right-hand terms approach a value of 1. Also, at small values of J_M , the numerator terms containing J_M become insignificant. When these constraints are applied and when $M_1 \gg M_8$ and $A_1 = A_2$, eq 14 reduces to eq 1. Therefore, the dependence of J_M on M_1 , L_T , and anion type correctly described by eq 1 is also correctly described by eq 14.

Equation 14 has at least two positive real roots. One set of roots correctly predicts the shape of the J_M vs. $\log K$ curves observed in our results. In Figure 5, the calculated J_M vs. $\log K$ curves are compared to the experimental data for K^+ , Rb^+ , Sr^{2+} , and Ba^{2+} transport. The following values for parameters in eq 14 were used to produce the theoretical curves shown in Figure 5. The values of L_T (1.0 mM), M_1 (1.0 M for K^+ , Rb^+ , and Sr^{2+} and 0.30 M for Ba^{2+}), and A_1/A_2 (0.245) were those used in the experimental procedure. A median value for M_8 was taken to be 1.0 mM. The value of D_W (1.57×10^{-5} cm²/s) was taken from tables in Reid, Prausnitz, and Sherwood.²² The values of D_L (1.4×10^{-5} cm²/s) and D_1 (1.8×10^{-5} cm²/s) were estimated by using eq 15,²² where

$$D = 7.4 \times 10^{-8} (\phi M)^{1/2} T / \mu V^{0.6} \quad (15)$$

(22) Reid, R. C.; Prausnitz, J. M.; Sherwood, T. K. "The Properties of Gases and Liquids", 3rd ed.; McGraw-Hill: New York, 1977; pp 566-582.

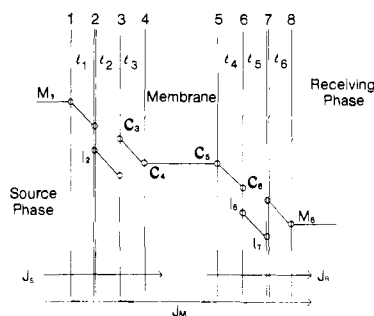


Figure 4. A theoretical representation of a liquid membrane system. Water and chloroform boundary layers are envisioned on each side of the membrane. The two chloroform boundary layers are each divided into two parts which, with the two water boundary layers, give six regions of thicknesses l_1 – l_6 . The limits of these regions are numbered 1–8. When used as subscripts, these last numbers serve to indicate the concentrations of M (metal ion), I (ion pairs), and C (cation-carrier complex associated with anions(s)) at each position.

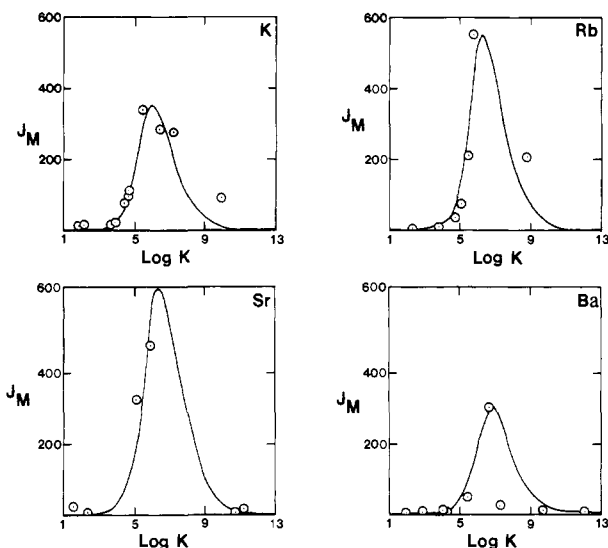


Figure 5. Plots of J_M vs. $\log K_{MeOH}$ for K^+ , Rb^+ , Sr^{2+} , and Ba^{2+} . The solid line represents the function given in eq 14. The points represent the experimental values.

ϕ is the association factor for chloroform (value used equal to 1), M is the molecular weight of chloroform (119.5), T is the temperature (298.2 K), μ is the viscosity of chloroform (0.55 centipoise), and V is the molar volume of ligand (300 cm^3/mol used as a representative value) or of the ion pair (200 cm^3/mol used as a representative value). The values of $l_1 = l_6$ and $l_3 = l_4$ were estimated by using the boundary layer equation (eq 16)²³ where

$$l = 4.64(vx/V)^{1/2}(\text{Sc})^{-1/3} \quad (16)$$

v is the kinematic viscosity (water = 10^{-2} cm^2/s ; chloroform = 3.7×10^{-3} cm^2/s), x is the distance from the center of stirring (0.45 cm), V is the undisturbed liquid velocity (8.2 cm/s), and Sc is the Schmidt number (water = 640; chloroform = 264). The value given by eq 16 for $l_1 = l_6$, 0.013 cm (using v for water), was used without modification because the shapes of the curves in Figure 5 were insensitive to the value chosen. The value for $l_3 = l_4$, 0.010 cm (using v for chloroform), was adjusted to 0.0048 cm to give the correct peak heights in Figure 5. The values of $l_2 = l_5$ were adjusted to give the best fits of the data, as shown in Figure 5: 2×10^{-5} cm (K^+); 5×10^{-6} cm (Rb^+); 2×10^{-6} cm (Sr^{2+}); 2×10^{-6} cm (Ba^{2+}). The values of l_2 and l_5 are a function of the ligand concentration and the kinetics of the association. Therefore this distance could well vary from cation to cation and

from ligand to ligand. Only one value was used for each cation. The values of l_2 and l_5 affect the shape of the curve more severely at high $\log K$ values. The values of k for each salt ($k_{K^+} = 3 \times 10^{-6}$ L/mol; $k_{Rb^+} = 2 \times 10^{-6}$ L/mol; $k_{Sr^{2+}} = 2 \times 10^{-6}$ (L/mol)²; $k_{Ba^{2+}} = 2 \times 10^{-6}$ (L/mol)²) were estimated to give the correct position of the curve maximum.

The position of the maximum in J_M vs. $\log K$ curves is largely governed by the value of k in this transport model. Among nitrate salts of alkali and alkaline earth cations, this value is expected to increase with cation size and to decrease with cation charge on the basis of the assumption that solvent interaction with these cations is almost purely of the ion-dipole type. This dependence predicts that the maximum should occur at higher $\log K$ values for divalent cations than for monovalent cations of similar size. The cations K^+ and Ba^{2+} are almost identical in size²⁴ and are interesting to compare in this light. As predicted, the highest observed transport for Ba^{2+} occurs at a $\log K_{MeOH}$ value (6.9) which is larger than that for K^+ (5.7). While the exact positions of the maxima in these curves are difficult to define on the basis of the data alone, the transport model lends weight to the argument that the apparent shift in the position of the maximum from the value for K^+ to a higher value for Ba^{2+} is real.

The variation in the amounts of salt partitioned into the membrane (as reflected in the value of k) among cations of the same charge is expected to be smaller than between cations of different charge. Thus, it is expected that variation in the position of the maximum among the monovalent or among the divalent cations will be too small to detect from our limited data.

As shown in Figure 5, the theoretical transport model predicts that the maxima in J_M vs. $\log K$ curves are not sharp, but rounded. If this is indeed the case, then a range of $\log K_{MeOH}$ values exists for each cation within which J_M is close to the value at the maximum. This range is approximately one $\log K_{MeOH}$ wide for monovalent cations (Figure 5). Since we have shown that for K^+ , the maximum must lie between $\log K_{MeOH}$ values 5.00 and 6.06, it is likely that the J_M value, 340, at $\log K_{MeOH}$ value 5.7 is close to the actual J_M value at the maximum proper. Since the maximum in the Rb^+ curve is expected to occur at a $\log K_{MeOH}$ value similar to that for K^+ (for reasons outlined above), the observed maximum J_M , 550, at $\log K_{MeOH}$ value 5.9 is also probably close to the true maximum value.

The diffusion model makes it possible to explain the drop in J_M with increasing $\log K$ at high $\log K$ values without involving the rate constant for complex dissociation (except as it reflects in the values of l_2 and l_5). As $\log K$ increases beyond a certain value, the amount of uncomplexed cation found in the membrane at the receiving phase interface, in the form of an ion pair, represented in Figure 4 by I_6 , decreases. Since the rate of diffusion across the membrane-receiving-phase interface (and hence the rate of accumulation of cation in the receiving phase) is governed by the differences in concentrations across the boundary layers at that interface, J_M decreases as I_6 decreases. Thus, the processes taking place at the receiving-phase interface are responsible for the trends in J_M at high $\log K$ values. Alternatively, at low $\log K$ values, the diffusion processes involved in uptake of the cation into the membrane exert the most influence on values of J_M .

The results and model presented above make possible the estimation of either J_M or $\log K$ in certain ranges if the other of the two values is known. Since the technique for measuring J_M is fast and simple and uses relatively small amounts of ligand, this method is especially desirable for estimating $\log K$, which is often difficult to obtain because of limited ligand solubility, the availability of only small amounts of ligand, and the amount of effort required to obtain $\log K$ data.

Acknowledgment. We are grateful to Dr. Jerald Bradshaw of Brigham Young University for providing samples of compounds 10–12 and to Dr. Edward M. Eyring of the University of Utah for helpful discussions.

(23) Bird, R. B.; Stewart, W. E.; Lightfoot, E. N. "Transport Phenomena"; Wiley: New York, 1960; pp 140–146.

(24) Shannon, R. D.; Prewitt, C. T. *Acta Crystallogr., Sect. B* 1969, B25, 925–946.